

Masthead Logo

Smith ScholarWorks

Geosciences: Faculty Publications

Geosciences

1-6-2009

Surface Cracks Record Long-Term Seismic Segmentation of the Andean Margin

John P. Loveless

Cornell University, jloveles@smith.edu

Richard W. Allmendinger

Cornell University

Matthew E. Pritchard

Cornell University

Jordan L. Garroway

Cornell University

Gabriel González

Universidad Católica del Norte

Follow this and additional works at: https://scholarworks.smith.edu/geo_facpubs

Part of the [Geology Commons](#)

Recommended Citation

Loveless, John P.; Allmendinger, Richard W.; Pritchard, Matthew E.; Garroway, Jordan L.; and González, Gabriel, "Surface Cracks Record Long-Term Seismic Segmentation of the Andean Margin" (2009). Geosciences: Faculty Publications, Smith College, Northampton, MA.

https://scholarworks.smith.edu/geo_facpubs/13

This Article has been accepted for inclusion in Geosciences: Faculty Publications by an authorized administrator of Smith ScholarWorks. For more information, please contact scholarworks@smith.edu

1 Surface cracks record long-term seismic segmentation of
2 the Andean margin

3 **John P. Loveless^{1,2}, Richard W. Allmendinger¹, Matthew E. Pritchard¹, Jordan L.**
4 **Garroway¹, Gabriel González³**

5 *¹Department of Earth and Atmospheric Sciences, Cornell University, Snee Hall, Ithaca,*
6 *New York 14853, USA*

7 *²Current address: Department of Earth and Planetary Sciences, Harvard University, 20*
8 *Oxford Street, Cambridge, Massachusetts 02138, USA*

9 *³Departamento de Ciencias Geológicas, Universidad Católica del Norte, Casilla 1280,*
10 *Antofagasta, Chile*

11 **ABSTRACT**

12 Understanding the long-term patterns of great earthquake rupture along a
13 subduction zone provides a framework for assessing modern seismic hazard. However,
14 evidence that can be used to infer the size and location of past earthquakes is typically
15 erased by erosion after a few thousand years. Meter-scale cracks that cut the surface of
16 coastal areas in northern Chile and southern Peru preserve a record of earthquakes
17 spanning several hundred thousand years owing to the hyperarid climate of the region.
18 These cracks have been observed to form during and/or shortly after strong subduction
19 earthquakes, are preserved for long time periods throughout the Atacama Desert,
20 demonstrate evidence for multiple episodes of reactivation, and show changes in
21 orientation over spatial scales similar to the size of earthquake segments. Our

22 observations and models show that crack orientations are consistent with dynamic and
23 static stress fields generated by recent earthquakes. While localized structural and
24 topographic processes influence some cracks, the strong preferred orientation over large
25 regions indicates that cracks are primarily formed by plate boundary-scale stresses,
26 namely repeated earthquakes. We invert the crack-based strain data for slip along the
27 well-known Iquique seismic gap segment of the margin and find consistency with gravity
28 anomaly-based inferences of long-term earthquake slip patterns, as well as the magnitude
29 and location of the November 2007 Tocopilla earthquake. We suggest that the meter-
30 scale cracks can be used to map characteristic earthquake rupture segments that persist
31 over many seismic cycles, which encourages future study of cracks and other small-scale
32 structures to better constrain the persistence of asperities in other arid, tectonically active
33 regions.

34 **INTRODUCTION**

35 The characteristic earthquake model of seismic recurrence suggests that a given
36 fault segment ruptures repeatedly in earthquakes of similar magnitude and areal extent
37 (Schwartz and Coppersmith, 1984). While some historical (Comte and Pardo, 1991) and
38 paleoseismic (Sieh, 1996) records support this model, it is unclear whether these seismic
39 segments are truly long-lived, because geologic indicators of distinct earthquakes usually
40 persist for only a few k.y. (up to ~10 events). To assess the longevity of the segmented
41 nature of seismicity, we require data that reflect deformation caused by 100s to 1000s of
42 repeated earthquakes.

43 Arrays of meter-scale surface cracks that penetrate coastal regions of the northern
44 Chile and southern Peru forearc provide insight into the long-term nature of great
45 earthquakes (magnitude 8 and larger) along the plate boundary. We use 2.5-m resolution
46 satellite imagery available in Google Earth to map concentrations of cracks throughout
47 the Andean forearc between 17.5° and 23.5°S (Fig. 1); examination of regions outside
48 these latitudinal bounds yields only sparse examples of cracking, likely due to slightly
49 wetter climatic conditions (Ewing et al., 2006) and presence of unconsolidated sediment
50 (Rech et al., 2003), both of which inhibit crack preservation. We complement the remote
51 sensing with field observations at several localities (Loveless, 2008; Loveless et al.,
52 2005) and, because cracks throughout the study area are morphologically similar, we
53 generalize our field results to regions we have not visited. In general, crack clusters show
54 preferred orientations that vary on spatial scales similar to great earthquake rupture areas.
55 Between 19° and 23°S, which mark the estimated latitudinal bounds of the great 1877
56 Iquique earthquake (Comte and Pardo, 1991), mean length-weighted crack strike rotates
57 from NW to NNE. At several localities including east of the Mejillones Peninsula (23°S),
58 there are populations of cracks showing a bimodal distribution in strike, with one set
59 striking NE and the other NW (Fig. 1). Cracks near Ilo, Peru strike at a high angle to the
60 coastline and plate boundary, approximately parallel to the direction of plate
61 convergence.

62 Hyperaridity in the region, which has persisted for at least the last 6 M.y. (Hartley
63 and Chong, 2002), if not since before 16–18 Ma (Dunai et al., 2005; Rech et al., 2006),
64 allows for long-term preservation of the cracks. The gypsum-indurated soil that covers

65 much of the coastal region between elevations of 300 and 1200 m (Rech et al., 2003)
66 provides a durable surface crust that further enhances crack preservation. Our field
67 observations reveal crack apertures ranging from 10s of cm to more than 1 m; these
68 cracks can be mapped using the imagery, but we cannot comprehensively define their
69 apertures. Although many cracks are preserved in the gypsum-indurated crust (Fig. 1,
70 inset), there are numerous fissures penetrating up to 12 m into bedrock. We interpret the
71 numerous layers of gypsum plated vertically onto crack walls as indication of repeated
72 episodes of sealing and reopening. The rate of gypsum accumulation is unknown,
73 limiting the information that it can provide about the age of cracks. However, based on
74 cosmogenic dating of the geomorphic surfaces into which the cracks cut and
75 morphologically similar neotectonic structures (González et al., 2006), we propose that
76 the cracks represent deformation as old as several hundred k.y., encompassing 1000s of
77 ~100 yr interplate earthquake cycles (Loveless et al., 2005).

78 Local structural, topographic, and/or geomorphic effects and stresses related to
79 earthquakes within the subducting slab (Marquardt et al., 2006) influence formation of
80 some cracks. In particular, some cracks strike parallel to crustal faults (González et al.,
81 2008) and drainages (Keefer and Moseley, 2004), indicating that pre-existing linear
82 features can affect crack strike. However, the large scale patterns of strike change (Fig.
83 1) and the fact that cracks were generated by the 1995 M_w 8.1 Antofagasta, Chile
84 (González and Carrizo, 2003) and 2001 M_w 8.5 Arequipa, Peru events (Keefer and
85 Moseley, 2004) indicate that interplate earthquakes are the principal driver of formation.
86 Mode 1 cracks – which, based on the paucity of observed lateral offset, we infer most

87 cracks to be (Loveless et al., 2005) – open in the direction of least compressional
88 principal stress (σ_3) and therefore strike parallel to the most compressional direction (σ_1)
89 (Pollard and Segall, 1987). By constructing a regional map of crack strikes, we
90 effectively map the orientations of the principal stress axes responsible for their
91 formation. The stress field produced by a subduction zone earthquake varies as a function
92 of the slip distribution on the fault, with σ_1 axes varying from nearly parallel to the fault
93 slip vector around the center of the rupture zone to oblique to the slip direction near the
94 rupture terminations (Fig. 2).

95 **MODELING COSEISMIC STRESS FIELDS**

96 In order to explore the relationships between the mode 1 surface cracks and plate
97 boundary earthquakes, we calculate the coseismic principal deviatoric stress fields related
98 to great earthquakes on four segments of the Andean margin: the 2001 Arequipa, 1868
99 $M\sim 8.5$ southern Peru, 1877 $M\sim 8.5$ Iquique, Chile, and 1995 Antofagasta events (rupture
100 areas shown in Figure 1; Detailed discussion appears in data repository¹). We use
101 published solutions for slip distributions of the 1995 (Pritchard et al., 2006) and 2001
102 (Pritchard et al., 2007) events and approximations of the historical earthquake slip
103 patterns (Comte and Pardo, 1991). Figs. DR1-DR4 illustrate the relationships between the
104 forward models of coseismic static stress fields and the permanent strain demonstrated by
105 the surface cracks.

106 In general, there is good agreement between the observed mean strikes of cracks
107 and the orientation of modeled σ_1 axes. In the case of the bimodal strike crack
108 populations east of the Mejillones Peninsula, we find that the NW striking cracks are

109 consistent with the NE-SW directed σ_3 axes induced by events on the Antofagasta
110 segment (Fig. DR1), while the NE striking cracks are opened by the NW-SE trending σ_3
111 axes related to seismicity on the Iquique segment (Fig. DR2). Similarly, the bimodal
112 crack clusters in northernmost Chile are affected by stress related to earthquakes on the
113 Iquique and southern Peru segments of the margin (Figs. DR2, DR3).

114 The rotation of mean crack strike from NNE to NW from south to north along the
115 length of the Iquique segment (Fig. 1) agrees with the stress field predicted by the
116 forward models (Figs. 2, DR2). The cracks mapped near the city of Ilo, Peru lie near the
117 center of the estimated rupture zone of the 1868 earthquake and strike nearly
118 perpendicular to the σ_1 orientation predicted by the 1868 model, indicating that these
119 cracks are minimally affected by the static stress caused by earthquakes on this segment,
120 on which the great 1604 earthquake also occurred (Comte and Pardo, 1991). The mapped
121 cracks are suggested to have formed either during or shortly after the 2001 Arequipa
122 earthquake (Keefer and Moseley, 2004). En echelon map patterns of these cracks suggest
123 accommodation of WSW-directed left-lateral shear in addition to opening, consistent
124 with the kinematics reported for nearby faults (Audin et al., 2008). This indicates that the
125 cracks near Ilo are mixed-mode (1 and 2) and thus we expect that σ_1 for the stress field
126 that created them should be oblique to the crack strike as predicted by our model of the
127 2001 event (Fig. DR4).

128 **INVERTING CRACK DATA FOR PALEOSEISMIC SLIP**

129 Studies of historical seismicity have relied on qualitative written records of
130 sustained damage (Comte and Pardo, 1991) to estimate event magnitude and location.

131 Given the agreement between predicted stress fields and observed crack strikes, we
132 propose that cracks can provide quantitative constraints on the slip distribution of paleo-
133 earthquakes. Because the inferred rupture limit of the 1877 earthquake encompasses 16
134 of the 17 cracked regions, we use the cracks to invert for plausible slip distributions
135 related to that event, or a sum of events occurring on the segment. In doing so, we make
136 the assumption that cracks used to constrain the slip pattern open exclusively due to
137 coseismic stress earthquakes on this segment, plus a contribution from regional stress
138 (see text in data repository).

139 The mean residual magnitude between the observed crack strikes and those
140 predicted by our preferred inversion is 8.2° (Fig. 3). While the solution for coseismic slip
141 is non-unique (see text in data repository), several robust features are notable. The
142 greatest resolved slip is concentrated ~ 35 km deep offshore Iquique (20.25°S), consistent
143 with the depth of maximum slip during the 1995 earthquake and $\sim 1^\circ$ north of the
144 epicenter of the 1877 earthquake inferred from historical data (Comte and Pardo, 1991).
145 Smaller loci of moment release are located around 22.5°S and 23.5°S . The distance
146 between slip patches suggests that they may represent separate earthquakes or widely
147 spaced asperities that rupture during a single event. Because of the lack of temporal
148 information contained in the data set, the crack-based strain field cannot distinguish a
149 single earthquake with a heterogeneous slip distribution from several smaller events.
150 Based on aftershocks mapped by the United States Geological Survey, the November
151 2007 M_w 7.7 Tocopilla earthquake ruptured the margin between $\sim 22^\circ$ and 23°S (Fig. 3),
152 indicating that it broke a portion of the plate boundary on which little Iquique event slip

153 is predicted by the inversion. This suggests that much of the segment ruptures during
154 truly great earthquakes such as that of 1877 but the portions remaining unbroken slip in
155 smaller events.

156 **DISCUSSION**

157 Recent studies (Llenos and McGuire, 2007; Song and Simons, 2003; Wells et al.,
158 2003) have found a correlation between negative forearc trench-parallel gravity
159 anomalies (TPGA) and zones of large-magnitude slip during strong subduction zone
160 earthquakes. We construct a TPGA (Sandwell and Smith, 1997; Song and Simons, 2003)
161 field for the Iquique segment to compare with the slip distribution resolved from our
162 inversion of the crack-based strain data (Fig. 3). The region in which resolved slip is
163 greatest coincides with an area of strongly negative TPGA. The lack of resolved slip at
164 shallow depths south of 21°S and occurrence of the smaller Tocopilla earthquake near
165 22°S are consistent with the prevalence of positive TPGA, which predicts slip of lower
166 magnitude during the characteristic Iquique event. The forearc gravity field is not a
167 transient property, thus both the gravity field and our inversion of geological data place
168 constraints on long-term patterns of great earthquake slip.

169 In addition to the static stresses, dynamic stresses associated with the passage of
170 seismic waves can also cause cracking of the surface (Dalguer et al., 2003). We calculate
171 the temporal evolution of stress induced at the surface by the 1995 and 2001 earthquakes
172 and find that stress axes calculated from static dislocation models are reasonably similar
173 in orientation to the dynamic principal stresses (Fig. DR7). This indicates that our
174 regional-scale mapping of cracks places constraints on the extent and distribution of slip

175 associated with plate boundary earthquakes, regardless of whether static or dynamic
176 stress is the primary driver of crack evolution. The method used to calculate dynamic
177 stress (Cotton and Coutant, 1997) does not take into account changes in material
178 properties such as the presence of existing faults and lithologic heterogeneity that may
179 localize deformation. We suggest that dynamic stressing is responsible for the formation
180 of the cracks near Antofagasta, which formed in poorly consolidated sediments parallel to
181 a nearby NE-striking fault scarp during the 1995 event (González and Carrizo, 2003) and
182 may have been impacted by the soil characteristics and fault structure.

183 We suggest that great earthquakes along the northern Chile and southern Peru
184 margin repeatedly rupture areas several hundred km in length in quasi-characteristic
185 earthquakes. If the location of segment boundaries varied substantially on hundred k.y.
186 timescales, we would expect cracks to show a range of strikes rather than one or two
187 preferred orientations, or a greater frequency of lateral offset. Historic records show that
188 not all segments completely re-rupture in single earthquakes but may sometimes break in
189 several smaller events (Kanamori and McNally, 1982). However, our models of
190 earthquake slip and crack formation indicate that on a regional scale, the stress field is
191 more sensitive to the extent of slip than details of its distribution (Fig. DR6). This
192 suggests that earthquakes on a given segment of the plate boundary may vary in their slip
193 distribution, but the accumulated strain exhibited by surface cracks implies that the
194 dimensions and boundaries of characteristic earthquake rupture remain relatively
195 constant.

196 The existence of long-lived earthquake segments has several implications.
197 Knowledge of segment dimensions and boundary locations is important for determining
198 earthquake recurrence intervals and thus assess seismic hazard. Numerous explanations
199 for the segmented nature of subduction zone earthquakes have been proposed, including
200 topographic features on the slab, interaction with upper plate faults (Audin et al., 2008),
201 and changes in upper plate structure, and our suggestion that segments are long-lived and
202 can be mapped by surface features will provide important constraints on these
203 hypotheses. Finally, surface cracks have been observed to form coseismically in
204 numerous tectonic settings, including along strike-slip faults on the Tibetan Plateau (Bhat
205 et al., 2007) and in the Middle East (Fielding et al., 2005), and our work motivates large-
206 scale mapping of these features using high-resolution global imagery, such as that
207 available in Google Earth, to determine whether long-lived seismic segmentation exists in
208 these and other areas.

209 **ACKNOWLEDGMENTS**

210 This research is supported by NSF grants EAR-0337496 (to RWA) and EAR-
211 0738507 (to RWA and MEP) and a NASA graduate research fellowship (NNG-04-
212 GQ-94-H, to JPL). Several figures were plotted using GMT (Wessel and Smith,
213 1991). We thank G. Hilley and D. Keefer for careful reviews, and B. Meade and F.
214 Maerten for helpful discussion.

215 **REFERENCES CITED**

216 Audin, L., Lacan, P., Tavera, H., and Bondoux, F., 2008, Upper plate deformation and
217 seismic barrier in front of Nazca subduction zone: The Chololo fault system and

- 218 active tectonics along the Coastal Cordillera, southern Peru: *Tectonophysics*, In
219 press, doi: 10.1016/j.tecto.2007.11.070.
- 220 Bhat, H., Dmowska, R., King, G.C.P., Klinger, Y., and Rice, J.R., 2007, Off-fault
221 damage patterns due to supershear ruptures with application to the 2001 M_w 8.1
222 Kokoxili (Kunlun) Tibet earthquake: *Journal of Geophysical Research*, v. 112,
223 B06301, doi: 10.1029/2006JB004425.
- 224 Comte, D., and Pardo, M., 1991, Reappraisal of great historical earthquakes in the
225 northern Chile and southern Peru seismic gaps: *Natural Hazards*, v. 4, p. 23–44, doi:
226 10.1007/BF00126557.
- 227 Cotton, F., and Coutant, O., 1997, Dynamic stress variations due to shear faults in a
228 plane-layered medium: *Geophysical Journal International*, v. 128, p. 676–688, doi:
229 10.1111/j.1365-246X.1997.tb05328.x.
- 230 Dalguer, L.A., Irikura, K., and Riera, J.D., 2003, Simulation of tensile crack generation
231 by three-dimensional dynamic shear rupture propagation during an earthquake:
232 *Journal of Geophysical Research*, v. 108, 2144, doi: 10.1029/2001JB001738.
- 233 Dunai, T.J., González L., G.A., and Juez-Larré, J., 2005, Oligocene–Miocene age of
234 aridity in the Atacama Desert revealed by exposure dating of erosion-sensitive
235 landforms: *Geology*, v. 33, p. 321–324, doi: 10.1130/G21184.1.
- 236 Ewing, S., Sutter, B., Owen, J., Nishiizumi, K., Sharp, W., Cliff, S.S., Perry, K., Dietrich,
237 W., McKay, C.P., and Amundson, R., 2006, A threshold in soil formation at Earth's
238 arid–hyperarid transition: *Geochimica et Cosmochimica Acta*, v. 70, p. 5293–5322,
239 doi: 10.1016/j.gca.2006.08.020.

- 240 Fielding, E.J., Talebian, M., Rosen, P.A., Nazari, H., Jackson, J.A., Ghorashi, M., and
241 Walker, R., 2005, Surface rupture and building damage of the 2003 Bam, Iran
242 earthquake mapped by satellite synthetic aperture radar interferometric correlation:
243 Journal of Geophysical Research, v. 110, B03302, doi: 10.1029/2004JB003299.
- 244 González, G., and Carrizo, D., 2003, Segmentación, cinemática y cronología relativa de
245 la deformación tardía de la Falla Salar del Carmen, Sistema de Fallas Atacama,
246 (23°40'S), norte de Chile: Revista Geológica de Chile, v. 30, p. 223–244.
- 247 **[[Q1: There is some discrepancy between "Gonzalez L." or just "Gonzalez."
248 Please choose one and make it consistent for all references to this author.
249 Q1]]**González, G., Dunai, T., Carrizo, D., and Allmendinger, R., 2006, Young
250 displacements on the Atacama Fault System, northern Chile from field observations
251 and cosmogenic ²¹Ne concentrations: Tectonics, v. 25, TC3006, doi:
252 10.1029/2005TC001846.
- 253 González, G., Gerbault, M., Martinod, J., Cembrano, J., Carrizo, D., Allmendinger, R.,
254 and Espina, J., 2008, Crack formation on top of propagating reverse faults of the
255 Chuculay Fault System, northern Chile: Insights from field data and numerical
256 modelling: Journal of Structural Geology, v. 30, p. 791-808, doi:
257 10.1016/j.jsg.2008.02.008.
- 258 Hartley, A.J., and Chong, G., 2002, Late Pliocene age for the Atacama
259 Desert: Implications for the desertification of western South America: Geology, v. 30,
260 p. 43–46, doi: 10.1130/0091-7613(2002)030<0043:LPAFTA>2.0.CO;2.

- 261 Kanamori, H., and McNally, K., 1982, Variable rupture mode of the subduction zone
262 along the Ecuador-Columbia coast: *Bulletin of the Seismological Society of*
263 *America*, v. 72, p. 1241–1253.
- 264 Keefer, D.K., and Moseley, M.E., 2004, Southern Peru desert shattered by the great 2001
265 earthquake: Implications for paleoseismic and paleo-El Niño-Southern Oscillation
266 records: *Proceedings of the National Academy of Sciences of the United States of*
267 *America*, v. 101, p. 10878–10883, doi: 10.1073/pnas.0404320101.
- 268 Llenos, A.L., and McGuire, J.J., 2007, Influence of fore-arc structure on the extent of
269 great subduction zone earthquakes: *Journal of Geophysical Research. Solid Earth*,
270 v. 112, B09301, doi: 10.1029/2007JB004944.
- 271 Loveless, J.P., 2008, Extensional tectonics in a convergent margin setting: Deformation
272 of the northern Chilean forearc [PhD. thesis]: Ithaca, NY, Cornell University.
- 273 Loveless, J.P., Hoke, G.D., Allmendinger, R.W., González, G., Isacks, B.L., and Carrizo,
274 D.A., 2005, Pervasive cracking of the northern Chilean Coastal Cordillera: New
275 evidence for forearc extension: *Geology*, v. 33, p. 973–976, doi: 10.1130/G22004.1.
- 276 Maerten, F., Resor, P., Pollard, D.D., and Maerten, L., 2005, Inverting for slip on three-
277 dimensional fault surfaces using angular dislocations: *Bulletin of the Seismological*
278 *Society of America*, v. 95, p. 1654–1665, doi: 10.1785/0120030181.
- 279 Marquardt, C., Naranjo, J.A., and Lavenu, A., 2006, Efectos geológicos del sismo del 13
280 de junio 2005, Región de Tarapacá, XI Congreso Geológico Chileno, Volume 2:
281 Antofagasta, Chile, p. 435–438.

- 282 Pollard, D.D., and Segall, P., 1987, Theoretical displacements and stresses near fractures
283 in rock: With applications to faults, joints, veins, dikes, and solution surface, *in*
284 Atkinson, B.K., ed., *Fracture Mechanics of Rock*: London, Academic Press, p. 277–
285 349.
- 286 Pritchard, M.E., Ji, C., and Simons, M., 2006, Distribution of slip from 11 $M_w > 6$
287 earthquakes in the northern Chile subduction zone: *Journal of Geophysical Research*,
288 v. 111, B10302, doi: 10.1029/2005JB004013.
- 289 Pritchard, M.E., Norabuena, E.O., Ji, C., Boroschek, R., Comte, D., Simons, M., Dixon,
290 T., and Rosen, P.A., 2007, Geodetic, teleseismic, and strong motion constraints on
291 slip from recent southern Peru subduction zone earthquakes: *Journal of Geophysical*
292 *Research*, v. 112, B03307, doi: 10.1029/2006JB004294.
- 293 Rech, J.A., Currie, B.S., Michalski, G., and Cowan, A.M., 2006, Neogene climate change
294 and uplift in the Atacama Desert, Chile: *Geology*, v. 34, p. 761–764, doi:
295 10.1130/G22444.1.
- 296 Rech, J.A., Quade, J., and Hart, W.S., 2003, Isotopic evidence for the source of Ca and S
297 in soil gypsum, anhydrite and calcite in the Atacama Desert, Chile: *Geochimica et*
298 *Cosmochimica Acta*, v. 67, p. 575–586, doi: 10.1016/S0016-7037(02)01175-4.
- 299 Sandwell, D.T., and Smith, W.H.F., 1997, Marine gravity anomaly from Geosat and ERS
300 1 satellite altimetry: *Journal of Geophysical Research*, v. 102, p. 10,039–10,054, doi:
301 10.1029/96JB03223.

- 302 Schwartz, D.P., and Coppersmith, K.J., 1984, Fault behavior and characteristic
303 earthquakes: Examples from the Wasatch and San Andreas fault zones: Journal of
304 Geophysical Research, v. 89, p. 5681–5698, doi: 10.1029/JB089iB07p05681.
- 305 Sieh, K., 1996, The repetition of large-earthquake ruptures: Proceedings of the National
306 Academy of Sciences of the United States of America, v. 93, p. 3764–3771, doi:
307 10.1073/pnas.93.9.3764.
- 308 Song, T.-R.A., and Simons, M., 2003, Large trench-parallel gravity variations predict
309 seismogenic behavior in subduction zones: Science, v. 301, p. 630–633, doi:
310 10.1126/science.1085557.
- 311 Wells, R.E., Blakely, R.J., Sugiyama, Y., Scholl, D.W., and Dinterman, P.A., 2003,
312 Basin-centered asperities in great subduction zone earthquakes: A link between slip,
313 subsidence, and subduction erosion?: Journal of Geophysical Research, v. 108, 2507,
314 doi: 10.1029/2002JB002072.

315 FIGURE CAPTIONS

316 **Figure 1.** Map of the northern Chile and southern Peru forearc regions. Ovals indicate the
317 approximate rupture segments of the most recent earthquakes on four segments of the
318 plate boundary; large dots represent the inferred epicenters. Rose diagrams show the
319 length-weighted distribution of crack strikes, with the black vector denoting the mean
320 strike. Inverted triangles show the position of the population; filled symbols denote
321 bimodal distribution in strike (see data repository). The dark gray region onshore shows
322 the area lying between 300 m and 1200 m elevation, delineating the bounds within which
323 gypsum precipitates from the dense coastal fog (Rech et al., 2003). The inset IKONOS

324 satellite image in the upper right corner shows an example of surface cracking. Cracks
325 are concentrated in gypsum-indurated sediment and are identified as parallel, N-S striking
326 dark lines in the light colored sediment. The darker regions are unconsolidated sediments
327 in which cracks are not well preserved.

328 **Figure 2.** Schematic relationship between subduction zone earthquake rupture area
329 (offshore ellipse with bold arrows denoting the coseismic slip vector) and principal stress
330 exerted at the surface. Gray arrows show σ_3 axes, which are approximately parallel to the
331 slip vector near the center of the rupture segment, opening cracks (narrow white ovals)
332 that strike in a perpendicular direction, parallel to the σ_1 direction (black axes). Near the
333 rupture terminations, cracks strike oblique to the earthquake slip vector.

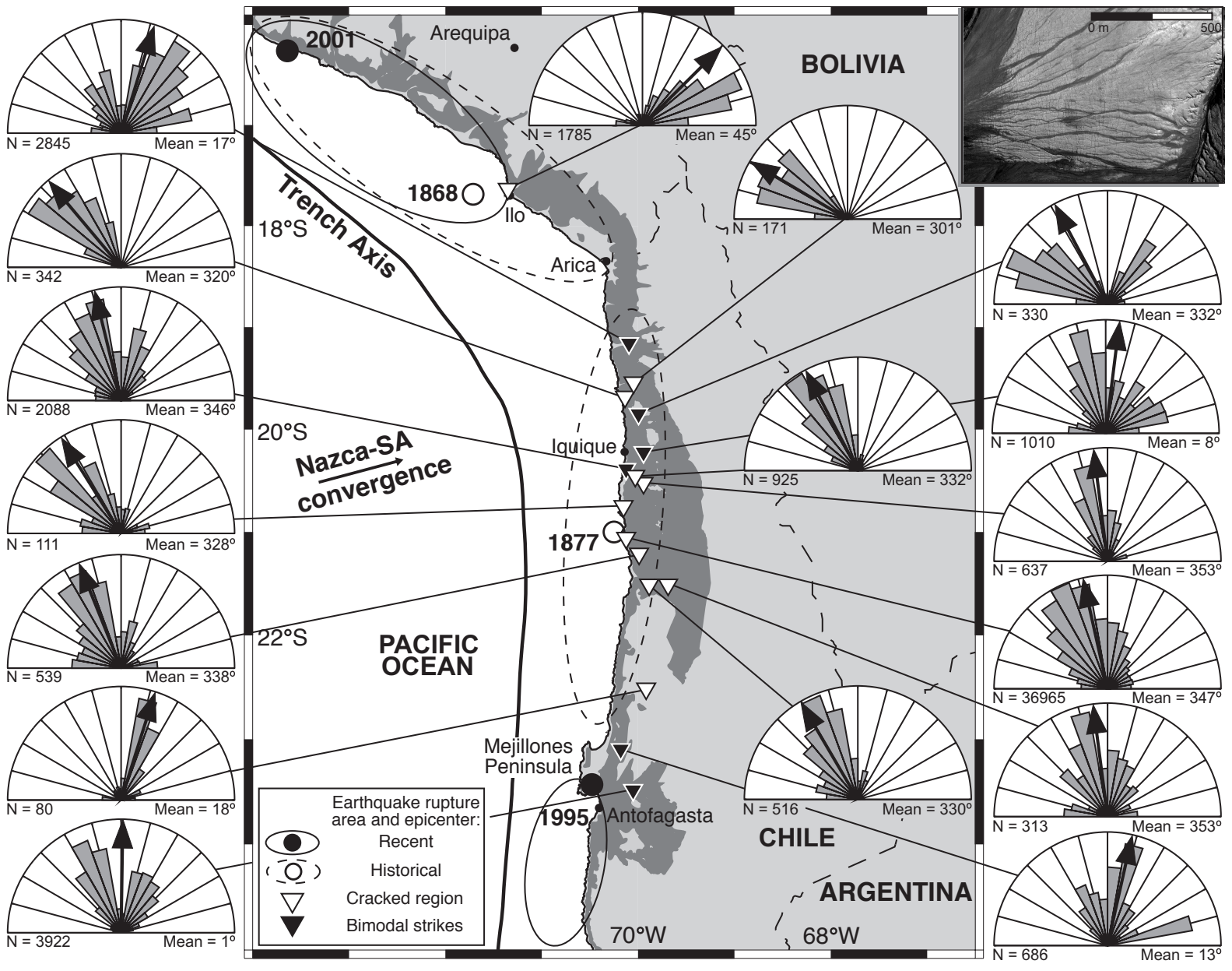
334 **Figure 3.** Preferred inverse model of the 1877 Iquique earthquake, shown as 1 m interval
335 contour lines of coseismic slip. The slip distribution was calculated by inverting (Maerten
336 et al., 2005) the strain field represented by the populations of surface cracks for slip on
337 the subduction interface. The mean crack strike at each mapped locality is shown by a red
338 bar and the calculated σ_1 orientation at the same location is indicated by a blue bar; the
339 mean residual angle between the observed and predicted crack strike is 8.2°. The contours
340 are overlain on the trench-parallel gravity anomaly (TPGA) constructed for the Iquique
341 segment. The region of greatest resolved slip for the Iquique event coincides with
342 strongly negative TPGA, consistent with recent studies (Llenos and McGuire, 2007; Song
343 and Simons, 2003; Wells et al., 2003). The approximate rupture area of the November
344 2002 M_w 7.7 Tocopilla earthquake is shown as the dashed rectangle, based on
345 information from the United States Geological Survey.

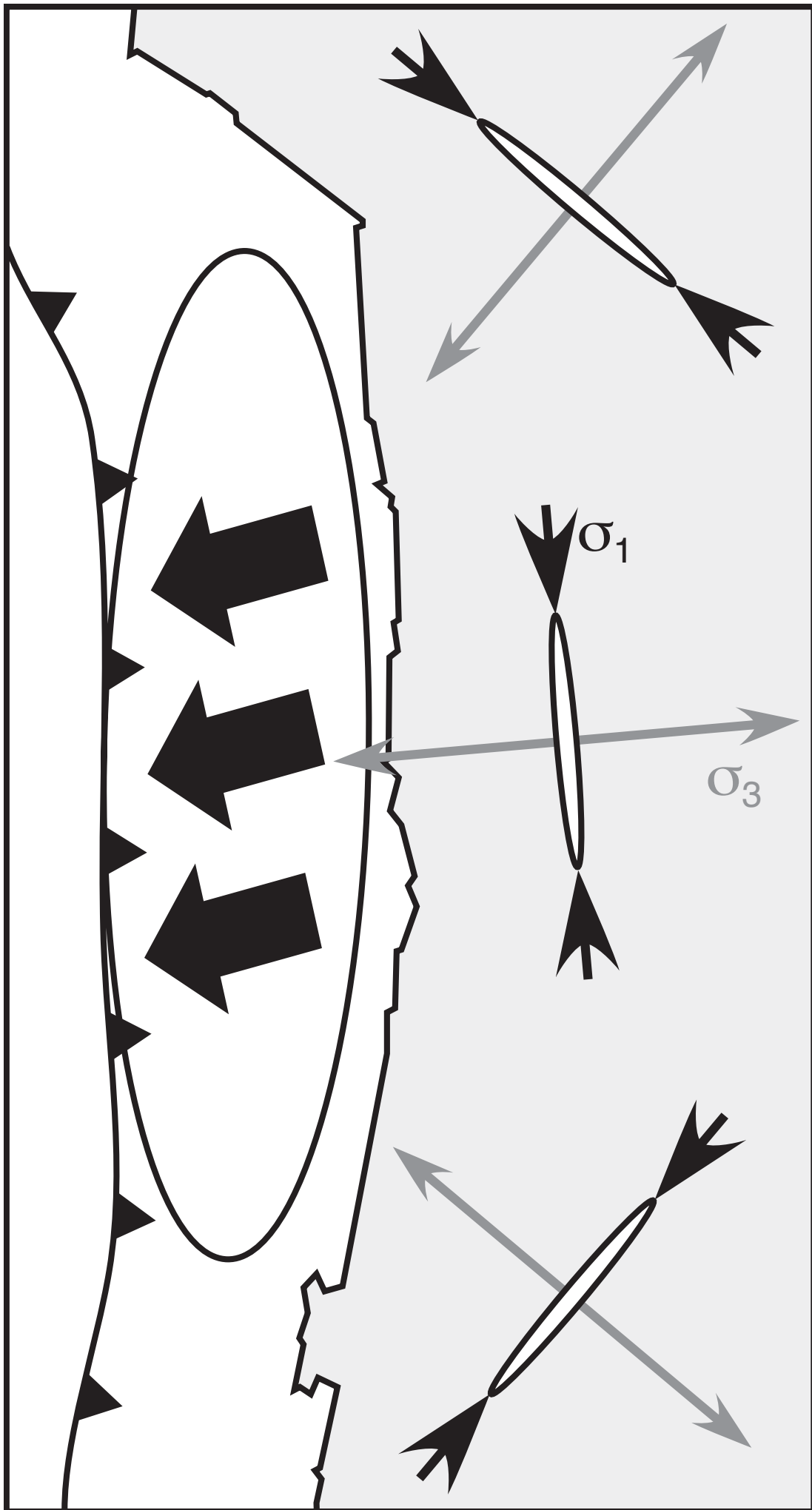
346 ¹ Data repository contains supplementary text, 7 figures, 3 tables.

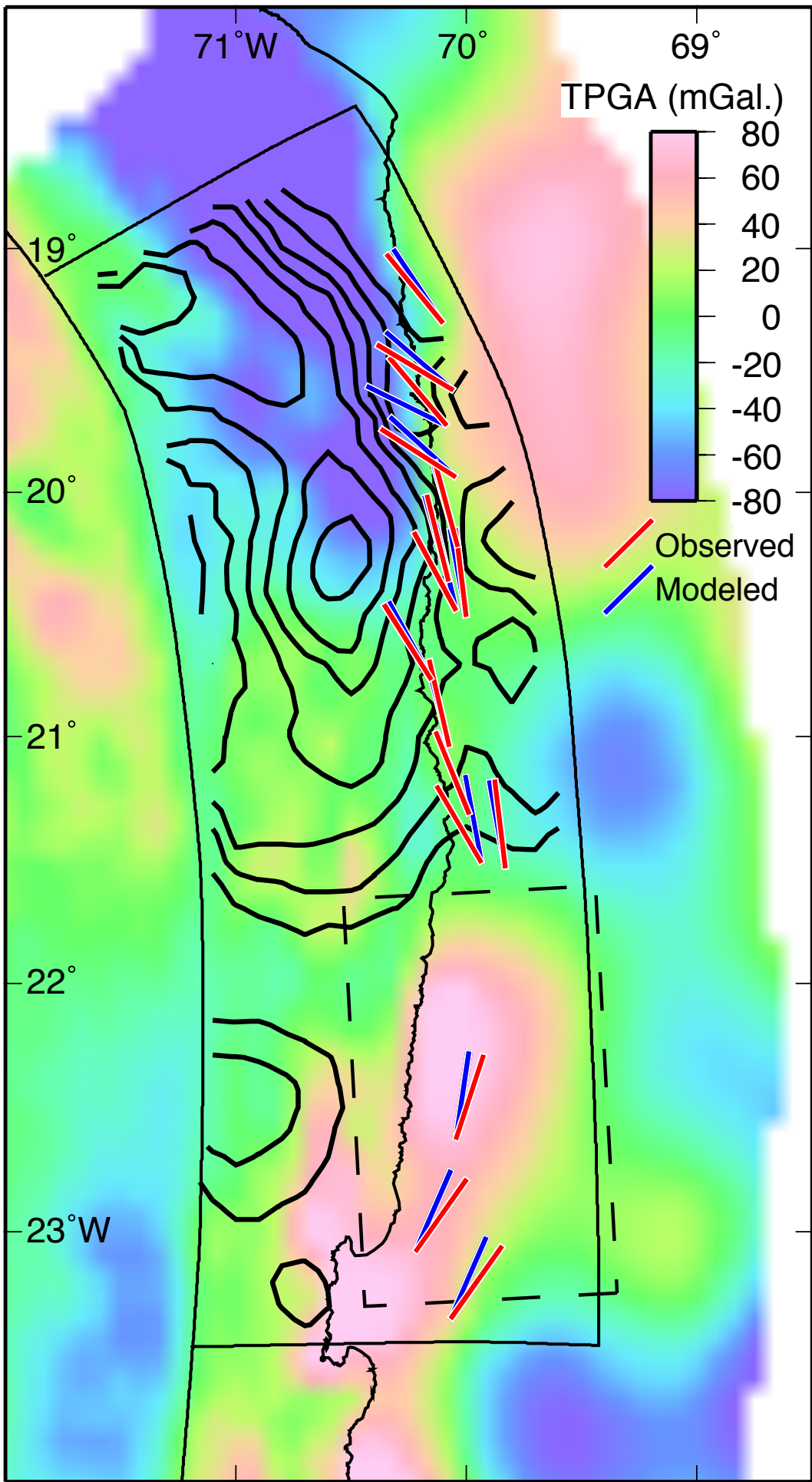
347 ²GSA Data Repository item 2008xxx, xxxxxxxx, is available online at

348 www.geosociety.org/pubs/ft2008.htm, or on request from editing@geosociety.org or

349 Documents Secretary, GSA, P.O. Box 9140, Boulder, CO 80301, USA.







Min./Max./Mean Angular Error: 0.8/8.2/23.4

Total Angular Error: 131